Multi-Fidelity Optimization with High-Fidelity Analysis and Low-Fidelity Gradients

Vladimir O. Balabanov (vladimir@vrand.com) * and Gerhard Venter (gventer@vrand.com) †
Vanderplaats Research and Development, Inc.
1767 South 8th Street
Colorado Springs, CO 80906

The paper introduces a new approach to multi-fidelity optimization. The approach employs gradient-based optimization, where the one-dimensional search points are evaluated using high-fidelity analysis, while the gradients are evaluated using low-fidelity analysis. Correlation between the results of the high- and low-fidelity analyses is not required. The approach is demonstrated using two example problems. Computational savings in terms of time and the number of high-fidelity analyses are discussed.

I. Introduction

ONE of the obstacles in practical implementation of optimization in industry is a potential high computational cost. An analysis of a complex system may take several hours and even days to complete and optimization requires performing many of these analyses. The number of design variables in optimization directly affects the number of analyses: the more design variables in the problem, the more analyses should be performed. This is especially true for a gradient-based optimization, where the gradients are evaluated using finite-difference calculations. A partial answer to the computational cost problem is Response Surface optimization methods[1-7,12], which do not require gradient information for optimization, thus reducing the required number of analyses. One difficulty with the Response Surface optimization methods is that their range of application is typically limited by about 20 design variables.

Another approach to reducing the computational cost is multi-fidelity optimization methods[8-12]. These methods combine high and low-fidelity analyses. One example of employing multi-fidelity optimization is creating a response surface from a relatively small number of high-fidelity analyses, then performing low-fidelity analyses for the same points and creating a response surface for low-fidelity analyses. Next, a correction factor is introduced that helps converting low-fidelity analysis results into the high-fidelity analysis results. The correction may be done for the response surfaces or for the analysis results themselves. Finally, when optimization is performed using the low-fidelity analysis, the results of each low-fidelity analysis is updated using the obtained correction factor. At some intermediate stage of the optimization and at the optimum a high-fidelity analysis is performed to verify the results. If the correlation is not satisfactory, the response surfaces for high and low-fidelity analyses are recreated and the correction factor is reevaluated. The process may be repeated several times. And the correction factor itself may constitute a response surface[12]. One of the disadvantages of this approach is that the results of high and low-fidelity analyses have to be correlated periodically during the course of optimization. For a relatively large number of design variables and responses the correlation may become rather involved, particularly, if each response employs its own correction factor, bringing up the limitation in the number of design variables and responses used.

The current paper proposes a modified approach to multi-fidelity optimization, where the one-dimensional search points in gradient-based optimization are evaluated using high-fidelity analysis and the finite difference gradient calculations are performed using low-fidelity analysis. One of the advantages of the proposed approach is that with the proper selection of high and low-fidelity analysis models there is no need to correlate the *results* of the two during optimization. Another advantage is that such an approach removes the potential limitation on the number of design variables and responses employed in response surface based multi-fidelity optimization.

---

* Senior R&D Engineer, Senior AIAA Member
† VisualDOC Project Manager, AIAA Member

II. Description of the Proposed Approach

In spite of the many advances in various optimization methods, gradient-based based optimization still holds the leadership in the number of design variables and constraints that the optimizer can handle. We tried to make use of existing gradient-based optimization methodology for optimizing models that require a lot of computational resources to be analyzed.

The proposed approach is based on the fact that for a robust gradient-based optimizer the gradients used in optimization potentially may be of relatively low quality, as long as the general direction of the gradient vector is captured correctly. The better the gradients, the easier it is for an optimizer to move around design space towards the optimum, but even with relatively low quality gradients a robust optimizer may bring the optimization process into a region of the actual optimum. Based on this observation we propose to employ two models during optimization: one of high fidelity and the other of low fidelity. The high-fidelity model will be used for analysis of the points in the one-dimensional search and the low-fidelity model will be used for calculating responses during the finite difference steps. The important aspect is that the design variables and responses present in the high-fidelity model and intended for use in optimization process must also be present in the low-fidelity model.

The underlying assumption in the proposed approach is that the designer will create two similar models and the low-fidelity model will approximately capture the behavior of the high-fidelity model. It is left up to the designer to decide how well the physics of both models should correspond to each other. One may argue that the results of the high-fidelity model analysis could be drastically different from the results of the low-fidelity model analysis and therefore the correlation between results is required. However, as long as the low-fidelity analysis captures the general trend of *changes* in responses due to *changes* in design variables, the differences in *absolute values* of responses may not be that important for a robust gradient-based optimizer. The reason is that during the finite difference gradient calculations the absolute values of the responses are not taken into account. The things that matter are the relative changes in the responses due to changes in the design variables. As long as these *relative changes* are approximately captured by a low-fidelity analysis, the finite difference gradient calculations should produce valuable gradient information.

The finite difference calculations are performed using the low-fidelity analysis, therefore the number of design variable and the number of responses involved in the optimization could be quite large. Also, the number of design variables and responses is not limited by the necessity to correlate the results obtained from high and low-fidelity analyses.

An example of a high-fidelity model could be a non-linear finite element structural analysis model in LS-Dyna[13] or ABAQUS[14] that may take many hours to run, while the corresponding model for a linear structural analysis in GENESIS[15], NASTRAN[16], or ABAQUS in the linear mode could take just minutes to run. Thus, from the computational cost standpoint the time spent on gradients calculations via linear structural analysis can be almost negligible in this case.

To summarize the main features of the proposed approach, here are the lists of its advantages and disadvantages.

Advantages:

- Makes it realistic to perform optimization with many design variables and responses using computationally expensive analysis by virtually eliminating the cost of the gradient calculations.
- Eliminates the need to correlate high and low-fidelity analysis results during optimization, when compared to more traditional multi-fidelity optimization methods.

Disadvantages:

- The designer has to create two models of different fidelity with the same design variables and responses. Here it is left up to the designer to be sure that the trends in the *changes* of the responses due to changes in the design variables are similar between the two models.
- It may become the responsibility of the designer to calculate the finite difference gradients using the low-fidelity analysis code, if there are no explicit gradient calculations present in the low-fidelity analysis code.
- The optimizer will most likely bring the design into the region of the optimum, rather than pinpointing the exact location of the optimum.

The ABAQUS finite element analysis code provides a partial solution to the problem of correlating linear and nonlinear models. After the nonlinear model is constructed, it is possible to make ABAQUS perform a linear analysis of the model by replacing just one keyword in the data deck.

An essential part of the proposed approach is a robust gradient-based optimization method, which in spite of the inaccurate gradients will be able to drive the design into the region of the optimum. A practical example of such an optimization method is the Modified Method of Feasible Directions inside of DOT[17] and VisualDOC[18] by Vanderplaats Research and Development, Inc.

III. Example Problems

A. Bending of a Curved Stepped Beam

As a first example problem for demonstrating the proposed approach we selected a problem of optimizing the shape of a curved beam, which can be a part of a 10-ton crane hook, shown in the Fig. 1.

Figure 1. The 10-ton crane hook

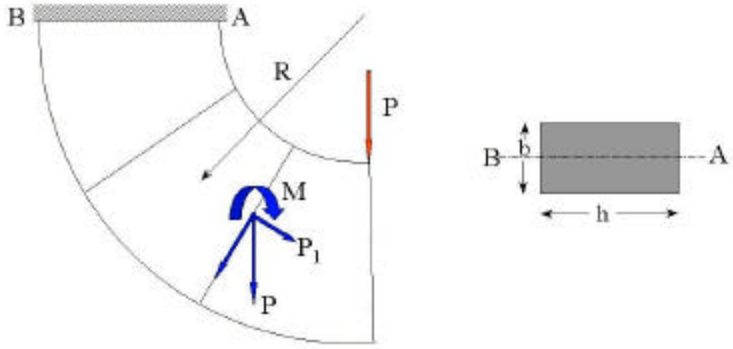

Figure 2. The curved beam divided into sections.

We optimized the lower left portion of the hook from Fig. 1 that included the points on the hook with the highest stress. We represented that portion of the hook as a curved beam divided into sections (Fig. 2).

To simulate the high-fidelity analysis, the maximum stress in the root of each section was calculated using the formula for bending stress in a curved beam[19], when the applied force, P, was resolved into a normal force, P_1, and a bending couple, M, for each section (the shear stresses were not considered):

$$s_A = \frac{P_1}{b*h} + \frac{M}{(b*h)*R}\left(1+\frac{1}{Z}\frac{h/2}{R-h/2}\right), \text{ where } Z = -1+\frac{R}{h}*\ln\left(\frac{R+h/2}{R-h/2}\right) \quad (1)$$

where h and b are the dimensions of the cross-section for each section.

To simulate the low-fidelity analysis we selected the model of a straight beam divided into the same number of sections as the curved beam (Fig. 3). The length of the straight beam was chosen to be equal to the radius of curvature, R, of the middle layer of the curved beam.

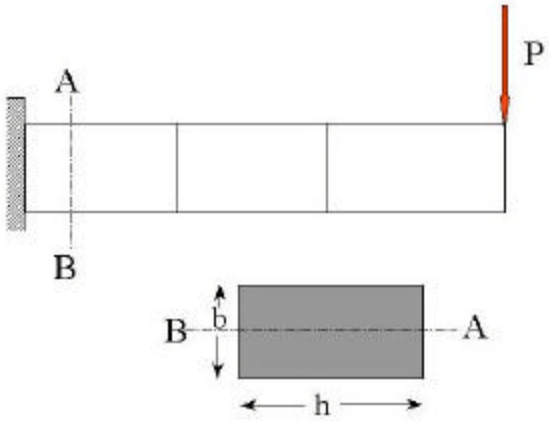

Figure 3. The straight beam divided into sections.

For the low-fidelity analysis the maximum stress in the root of each section was calculated using the formula for bending stress in a straight beam[19] (the shear stresses were not considered):

$$s_A = \frac{M * h}{\left(2 * \frac{b * h^3}{12}\right)}, \quad (2)$$

where again h and b are the dimensions of the cross-section for each section.

Although the two models (Figs. 2 and 3) were quite different, we felt that the model for the low-fidelity analysis correctly captures the general trends for *changes* in stresses and volume of the beam due to changes in design variables. As mentioned before, the important part was to be sure that the same responses were present in both the high- and low-fidelity models.

Table 1 presents the parameter values used for both models:

Table 1. Parameter values for the curved beam optimization problem.

Parameter Notation	Description	Value
P	Applied concentrated force	20,000 *lb*
R	Radius of the middle layer of the curved beam	4.5 *in*
h	*Initial* height of each segment	4.0 *in*
b	*Initial* width of each segment	2.0 *in*

The optimization goal was to minimize the volume, V, of the portion of the beam, subject to constraints on the maximum stresses, s_A, in each section: $s_A < 20{,}000$ *psi*. The cross-sections dimensions of each section, h and b, were the design variables. Section numbering started from the clamped end of each beam. To prevent singularities in calculating the stresses in each section additional geometrical constraints were introduced: $h < 20b$. The following bounds were used for the design variables: $0.5 \le h \le 8$, $0.5 \le b$. The optimization was performed using the Modified Method of Feasible Directions inside of the VisualDOC optimization system.

For benchmarking purposes the one-level optimization was performed first, where both one-dimensional search points and finite difference steps points were analyzed using high-fidelity analysis (curved beam formula). After that the multi-fidelity optimization was performed, where the one-dimensional search points were analyzed using high-fidelity analysis and finite difference steps points were analyzed using low-fidelity analysis (straight beam formula).

Two separate cases were considered to study how the number of design variables may affect the number of high-fidelity analyses. In the first case both straight and curved beams were divided into 5 sections and in the second case both straight and curved beams were divided into 30 sections. Thus, the first case had 10 design variables and 10 constraints, and the second case had 60 design variables and 60 constraints.

The results for the 5-section beam are as summarized in Table 2 and Figs. 4-7. Note, that in the history plots one iteration includes several points of one-dimensional search and finite difference calculations.

Table 2. Main results for the 5-section curved beam optimization problem.

Parameter	Initial Value	Optimum from Direct Optimization	Optimum from Multi-Fidelity Optimization
Volume (V)	56.55	49.73	51.38
The total number of high-fidelity analyses	–	185	69
The number of analyses for finite differences	–	45	25

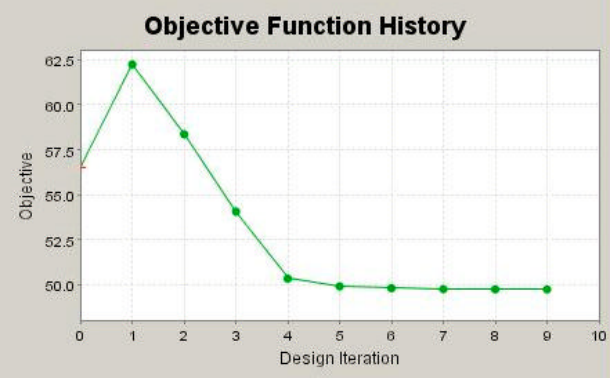

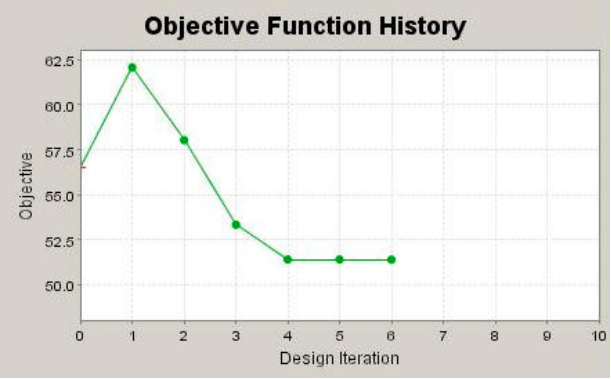

(a) Direct optimization **(b) Multi-fidelity optimization**

Figure 4. The objective functions history for direct and multi-fidelity optimization of a 5-section beam (Red star for the initial design designates one or more violated constraint)

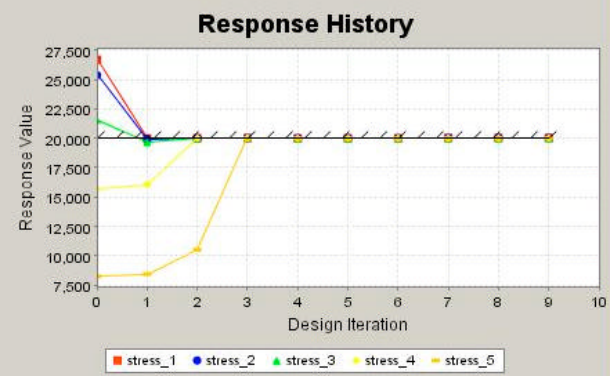

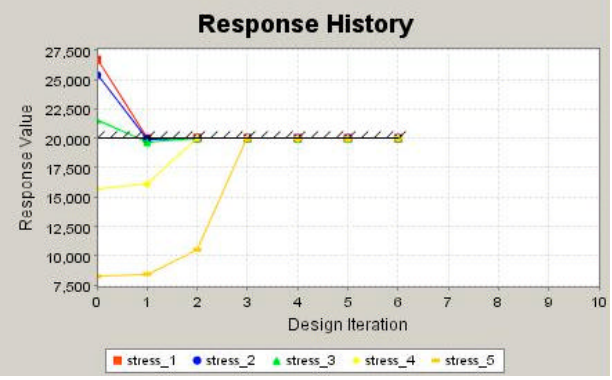

(a) Direct optimization **(b) Multi-fidelity optimization**

Figure 5. The stress constraints history for direct and multi-fidelity optimization of a 5-section beam

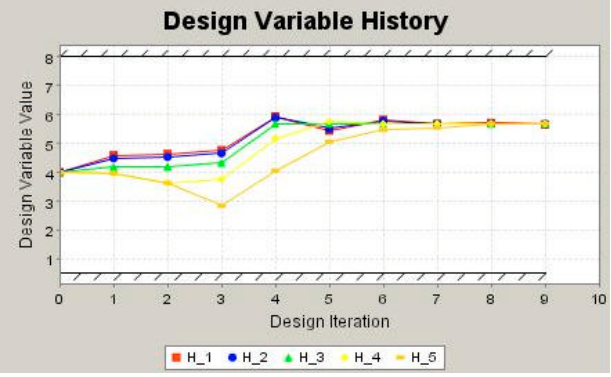

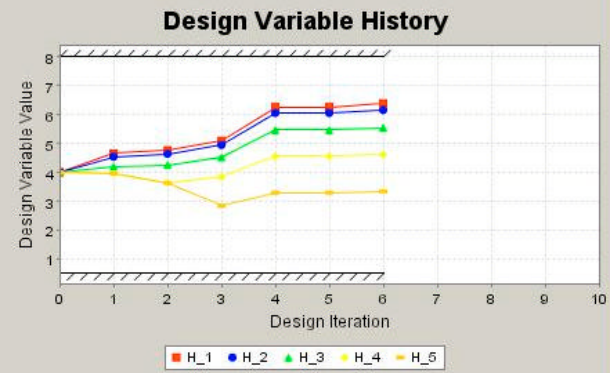

(a) Direct optimization **(b) Multi-fidelity optimization**

Figure 6. The cross-sectional height, *h*, history for each section for direct and multi-fidelity optimization of a 5-section beam

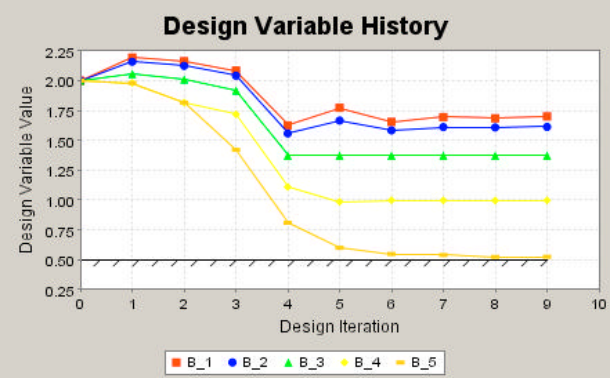

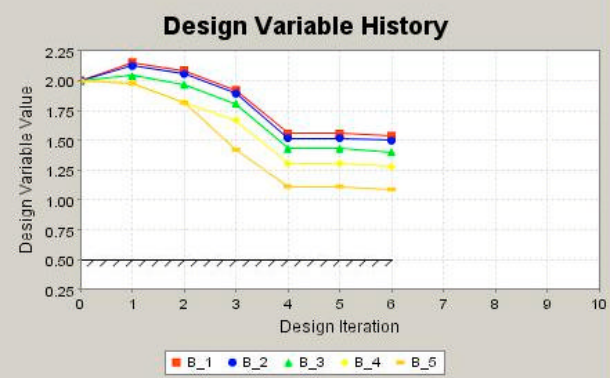

(a) Direct optimization **(b) Multi-fidelity optimization**

Figure 7. The cross-sectional width, *b*, history for each section for direct and multi-fidelity optimization of a 5-section beam

The results for the 30-section beam are summarized in Table 3 and Figs. 8-11.

Table 3. Main results for the 30-section curved beam optimization problem.

Parameter	Initial Value	Optimum from Direct Optimization	Optimum from Multi-Fidelity Optimization
Volume (V)	56.55	44.76	46.33
The total number of high-fidelity analyses	–	1397	159
The number of analyses for finite differences	–	600	510

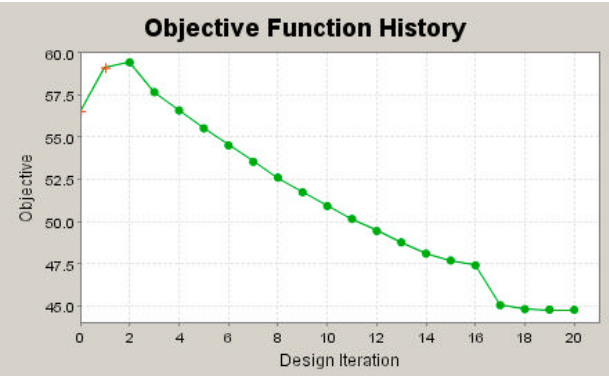

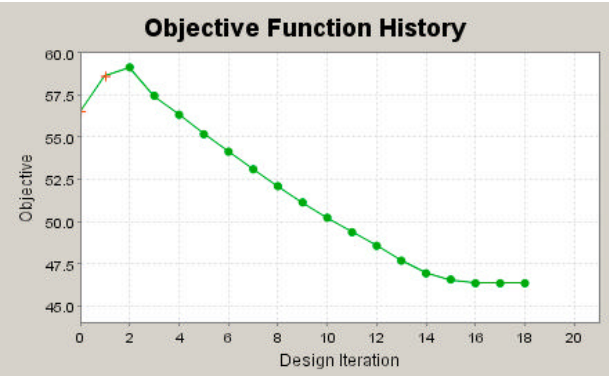

(a) Direct optimization **(b) Multi-fidelity optimization**

Figure 8. The objective functions history for direct and multi-fidelity optimization of a 30-section beam (Red star designates one or more violated constraint)

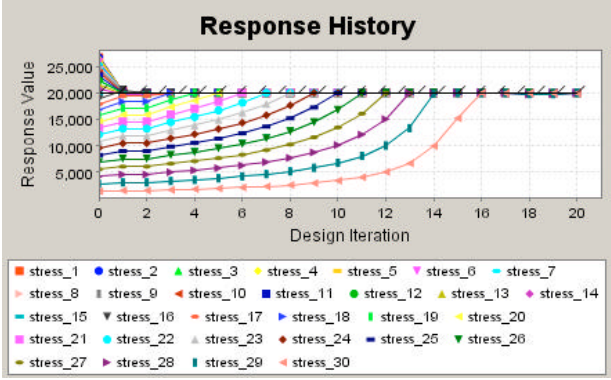

(a) Direct optimization

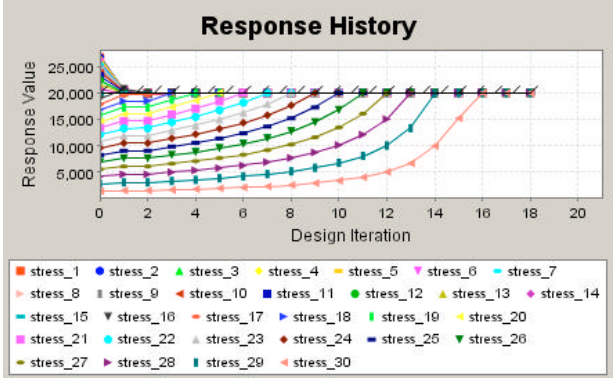

(b) Multi-fidelity optimization

Figure 9. The stress constraint history for direct and multi-fidelity optimization of a 30-section beam

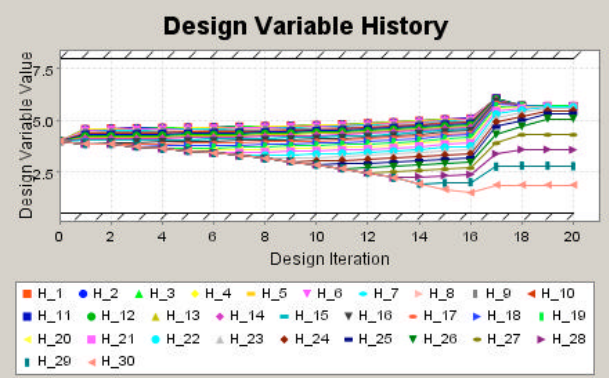

(a) Direct optimization

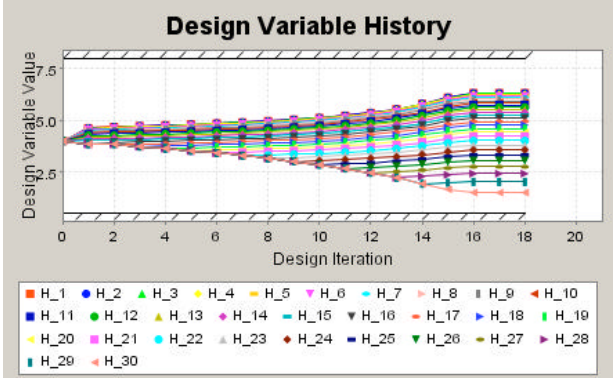

(b) Multi-fidelity optimization

Figure 10. The cross-sectional height, *h*, history for each section for direct and multi-fidelity optimization of a 30-section beam

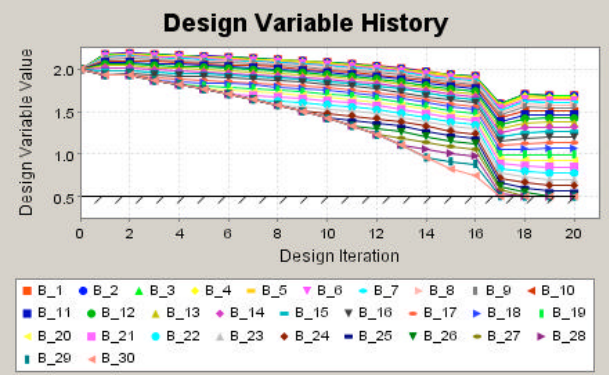

(a) Direct optimization

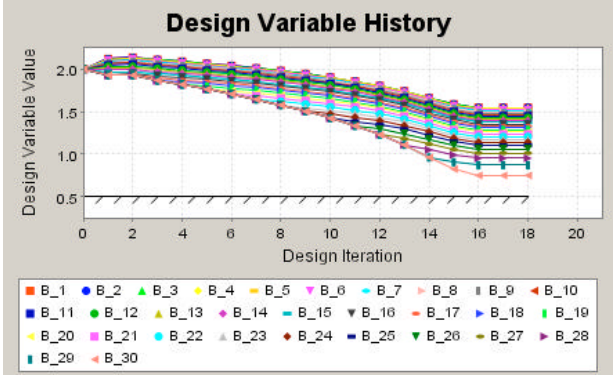

(b) Multi-fidelity optimization

Figure 11. The cross-sectional width, *b*, history for each section for direct and multi-fidelity optimization of a 30-section beam

We also compared the absolute values of the maximum stresses from the high- and low-fidelity analyses for the initial and final values of the design variables. The results are summarized in Table 4.

Table 4. Maximum stress values for various designs predicted by high- and low-fidelity analysis.

Analysis Type	Initial Design	Final Design of a Direct Optimization of a 5-segment Beam	Final Design of a Direct Optimization of a 30-segment Beam
Low-fidelity (straight beam)	24,375	14,364	14,223
High-fidelity (curved beam)	26,684	20,042	20,000

By analyzing the results of the optimization, it is possible to conclude that the proposed approach to multi-fidelity optimization was successful both for the case of relatively small and relatively large number of design variables. Although the results of the multi-fidelity optimization were not as good as the results of the direct optimization with high-fidelity analyses only, in both cases the final design of the multi-fidelity optimization was in the region of the optimum from the direct optimization.

The savings of the multi-fidelity optimization in terms of number of high-fidelity analyses performed were considerable for both optimization cases. For the case of a small number of design variables less than 50% of the high-fidelity analyses were required during multi-fidelity optimization compared to direct optimization. For the case of a large number of design variables less than 20% of the high-fidelity analyses were required during multi-fidelity optimization compared to direct optimization. Based on these results we may suggest that the most savings from this method could be expected for the problems with relatively large number of design variables, although problems with relatively small number of design variables also may result in considerable savings.

The multi-fidelity optimization approach worked in spite of the fact that the initial design was infeasible (some constraints were violated) and that at the end of optimization all the stress constraints were active. This may be attributed to the fact that our particular low-fidelity analysis was adequate in capturing the *changes* in the responses due to changes in the design variables, even though the difference in the absolute values of the stresses for the high- and low-fidelity analyses increased towards the end of optimization.

The number of high-fidelity analyses required for multi-fidelity optimization grows slower than linear with respect to the number of design variables in the optimization problem: for 5 design variables 69 high-fidelity analyses were required, whereas for 60 design variables 159 high-fidelity analyses were conducted. This observation gives a hope of performing optimization problems with a large number of design variables for computationally expensive analysis models.

B. Buckling of a Stiffened Plate

This optimization problem is based on a problem from the ABAQUS Example Problem Manual[20] and consists of a rectangular plate that is 10.8 *m* long and 6.75 *m* wide with a skin thickness of 5.00 *mm.* The plate is reinforced with several stiffeners in both the longitudinal and transverse directions (Fig. 12)

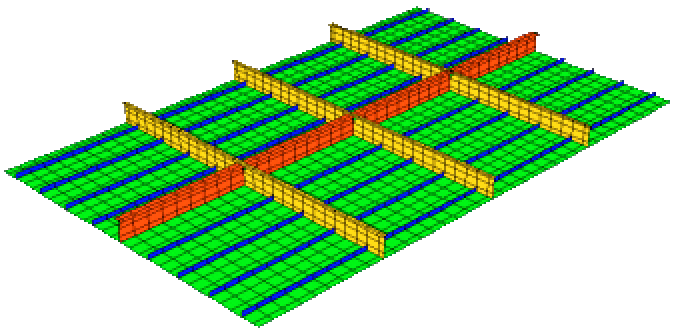

Figure 12. Stiffened Plate

The boundary conditions reflect the fact that the plate represents a part of a larger naval structure. Two longitudinal sides have symmetric boundary conditions, and two transverse (shorter) sides have pinned boundary conditions. In addition springs are located at two major reinforcement intersections, representing flexible conditions to the rest of the structure. The finite element mesh consists of 1,975 grid points and 2,214 elements: 1,912 S4 shell

elements, 14 S3 shell elements and 288 B31 beam elements. The structure is made of construction steel with an initial flow stress of 235 *MPa*.

The nonlinear analysis consists of two ABAQUS steps. In the first step a gravity load is applied perpendicular to the plane of the plate. In the second step a longitudinal compressive load of 6.46×10^6 *N* is applied to one of the pinned sides of the plate. All the nodes on that edge of the plate are forced to move in unison by means of multi-point constraints. The analysis is quasi-static, but buckling occurs. Initially, local out of plane buckling develops through the plate inside of each sections delimited by the reinforcements. Later, global buckling develops along a front of the section that is adjacent to the applied load (Fig. 13).

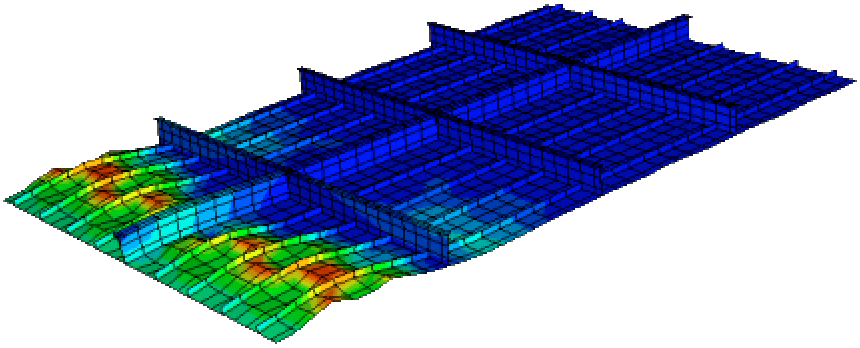

Figure 13. Buckling of a Stiffened Plate

In the optimization problem we redistribute the existing material of the plate to avoid buckling. This is achieved by minimizing the longitudinal displacement of the pinned (shorter) side of the plate where the load is applied, while maintaining the initial mass of the plate. The optimizer was allowed to add less than 2% to the initial mass of the plate: the mass constraint was set to 4700 *kg*, while the mass of the initial configuration is 4599 *kg*. The following seven design variables were considered: the skin thickness, web thickness of the main longitudinal stiffener, cap thickness of the main longitudinal stiffener , web thickness of the transverse stiffeners, cap thickness of the transverse stiffeners, web thickness of the small longitudinal stiffeners, and the side length of the square cross-sectional area of the cap of the small longitudinal stiffeners represented by beam elements. The lower and upper bounds on all the design variables are 1.0 *mm* and 100.0 *mm* respectively. The initial configuration was chosen to have the same dimensions as the original ABAQUS example problem. The initial parameter values are summarized in Table 5.

Table 5. Initial parameter values for the stiffened plate optimization problem.

Parameter Notation	Description	Value
skin	Thickness of the skin shell elements	5.0 *mm*
long stiff web	Thickness of the shell elements in the web of the small longitudinal stiffeners	6.0 *mm*
cross stiff web	Thickness of the shell elements in the web of the transverse stiffeners	7.0 *mm*
cross stiff cap	Thickness of the shell elements in the cap of the transverse stiffeners	10.0 *mm*
main stiff web	Thickness of the shell elements in the web of the main longitudinal stiffener	10.0 *mm*
main stiff cap	Thickness of the shell elements in the cap of the main longitudinal stiffener	10.0 *mm*
b2	Side length of the square cross sectional area in the cap of the small longitudinal stiffeners	15.0 *mm*

Two types of optimization were performed. At first for benchmarking purposes a one-level optimization was performed, where both the one-dimensional search points and the finite difference step points were analyzed using the non-linear analysis. Next, a multi-fidelity optimization was performed, where the one-dimensional search points were analyzed using the non-linear analysis and the finite difference steps points were analyzed using the linear

analysis. Both linear and non-linear analyses were performed in ABAQUS. The linear analysis was performed by changing one instruction in the ABAQUS data file for non-linear analysis. Thus, the difficulty of maintaining a separate model for a linear analysis was eliminated. One should note that in the case of the linear analysis the results of the first step (gravity loading) by definition do not influence the results of the second step (compressive load), because the loads from different steps are considered independent. Whereas in the case of non-linear analysis the first step loading has an influence on the second step. In spite of this difference we considered that the *relative changes* in design variables for the linear case still capture the general trends of the *relative changes* in the design variables for the non-linear case.

As in the case of the curved beam optimization problem, we chose to use the Modified Method of Feasible Directions optimization algorithm implemented in VisualDOC. The interaction between the optimizer and the ABAQUS analysis was implemented using VisualScript. VisualScript provides a graphical interactive interface between VisualDOC and any analysis program with ASCII input/output files.

The optimization results are summarized in Table 6 and Figs. 14-16. Note, that in the history plots one iteration includes several points of the one-dimensional search and the finite difference calculations.

Table 6. Main results for the stiffened plate optimization problem.

Parameter	Initial Value	Optimum from Direct Optimization	Optimum from Multi-Fidelity Optimization
Edge Displacement (mm)	77.0	8.0	7.0
Mass (kg)	4599.0	4687.2	4691.3
The total number of high-fidelity analyses	–	80	32
The number of analyses for finite differences	–	28	28

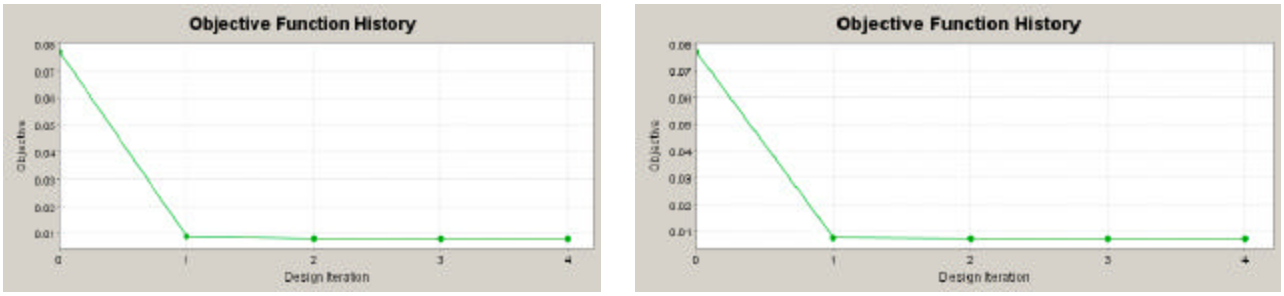

(a) Direct optimization **(b) Multi-fidelity optimization**

Figure 14. The objective functions history for direct and multi-fidelity optimization of a stiffened plate.

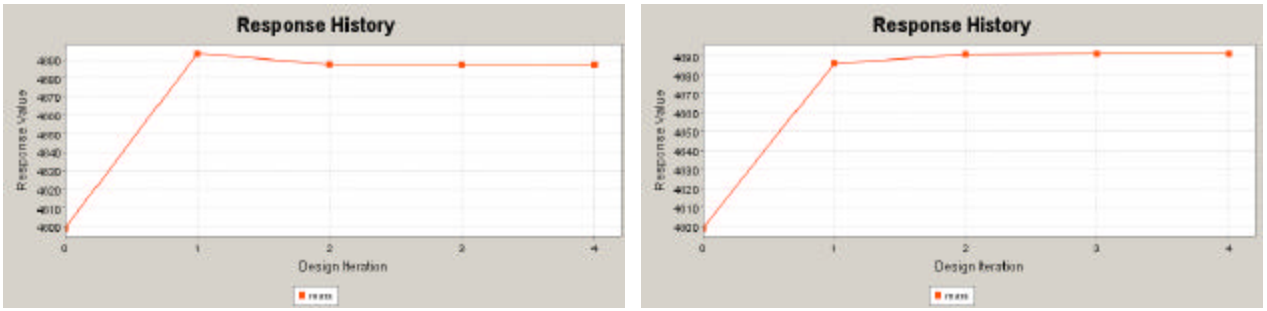

(a) Direct optimization **(b) Multi-fidelity optimization**

Figure 15. The mass constraints history for direct and multi-fidelity optimization of a stiffened plate.

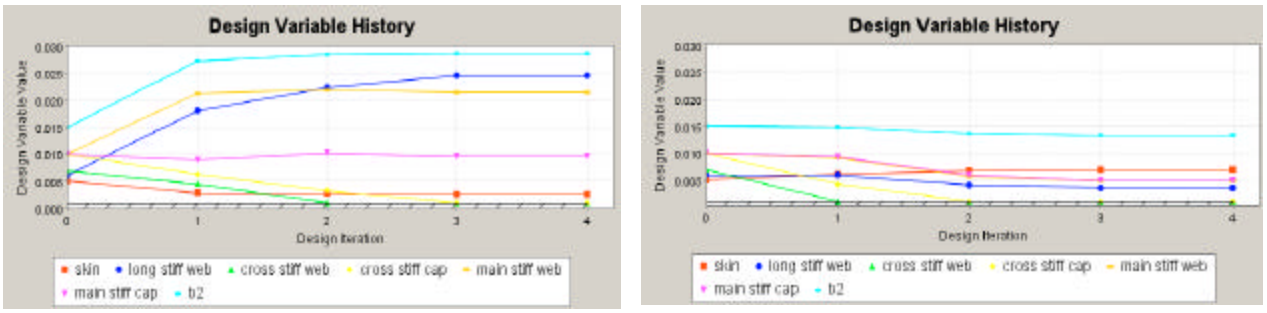

(a) Direct optimization **(b) Multi-fidelity optimization**

Figure 16. The design variable history for direct and multi-fidelity optimization of a stiffened plate.

By analyzing the obtained results we conclude that the proposed approach to multi-fidelity optimization was successful for the stiffened plate optimization problem. Both optimization procedures succeeded in eliminating buckling of the plate and reducing the displacements of the pinned (shorter) side under the compressive load by an order of magnitude. One can clearly see that the optimum configuration from the multi-fidelity optimization is quite different from the optimum configuration obtained by the direct optimization (Fig. 16). Although the objective (displacement) values are comparable for both optimizations. This may indicate relatively flat design space, when similar objective values could be achieved for various combinations of design variables. Referring to the physics of the problem, it is quite possible that one may redistribute the existing material in several ways, each of them providing similar displacements of the pinned (shorter) side under the compressive load.

Similarly to the bending of the curved beam problem, the savings of the multi-fidelity optimization in terms of number of high-fidelity analyses performed were considerable. Around 40% of the high-fidelity analyses were required during multi-fidelity optimization compared to direct optimization.

One has to note, however, that because of the iterative nature of the non-linear finite element analysis, different configurations of the same structure (e.g., with different thickness of shell elements) take different time to converge on the answer. It depends on the amount of non-linearity that the structure exhibits under the imposed load conditions. Because of that the wall-clock time savings were not as impressive for this optimization problem when compared to the savings in the number of non-linear analyses. The direct optimization required 14 hours and 7 minutes to complete (average time of about 10.6 minutes per analysis), while multi-fidelity optimization required 10 hours and 29 minutes (average time of 19.6 minutes per non-linear analysis if we disregard the time for the linear analyses). Such difference in average computational time may be explained by the fact that linear gradients drove the optimization procedure to the designs that took considerably longer time to converge in non-linear analysis. Even in such unfavorable conditions the wall-clock time savings of multi-fidelity optimization with respect to direct optimization still constitute around 25%.

IV. Conclusions

The method of multi-fidelity gradient-based optimization was developed and tested on two example problems. In this method the one-dimensional search points are analyzed using a high-fidelity analysis and finite-difference steps points are analyzed using a low-fidelity analyses. The method allows for using relatively large number of design variables and responses in optimization that involves computationally costly nonlinear (high-fidelity) analyses. At the same time the proposed approach eliminates the need for direct correlation of the results between the high- and low-fidelity analyses in the course of optimization. However, the method puts a responsibility on the designer to maintain both high- and low-fidelity models and to make sure that the trends in the *changes* of the responses due to changes in the design variables are similar between high and low-fidelity models. The designer may be also responsible for calculating gradients using the low-fidelity analyses, if this capability is not directly available in the chosen low-fidelity analysis code.

The essential feature of the proposed method is a robust gradient-based optimizer. An example of such an optimizer is DOT and VisualDOC from Vanderplaats Research and Development, Inc.

The proposed method gives a hope of performing optimization problems with a large number of design variables for computationally expensive analysis models.

The possible application of this multi-fidelity optimization method may include the optimization of non-linear structural models (e.g., in LS-Dyna or ABAQUS) when gradients are calculated using linear structural analysis codes, such as NASTRAN or GENESIS as well as using linear modes of non-linear codes themselves. CFD applications with corresponding high and low-fidelity analyses are also possible.

References

[1] Vanderplaats, G. N., "Approximation Concepts for Numerical Airfoil Optimization," NASA TP-1370, November 1978.

[2] Vanderplaats, G. N., "An Efficient Algorithm for Numerical Airfoil Optimization," AIAA J. Aircraft, Vol. 16, No. 12, December 1979, pp. 842-847.

[3] Redhe, M., Forsberg, J., Jansson, T., Marklund, P.-O., and Nilsson, L., "Using the Response Surface Methodology and the D-optimality Criterion in Crashworthiness Related Problems," *Structural and Multidisciplinary Optimization*, Vol. 24, pp. 185-194, 2002.

[4] Marklund, P., Nilsson, L., Rahmn, S., Jonsson, M., Svantesson, T. and Hellgren, L., "Optimization of a Press Hardened B-pillar by Use of the Response Surface Method," *SAE International Body Engineering Conference and Exposition*, Detroit, MI, Sep. 28-30, 1999.

[5] Avalle, M., Chiandussi, G., and Belingardi, G., "Design Optimization by Response Surface Methodology: Application to Crashworthiness Design of Vehicle Structures," *Structural and Multidisciplinary Optimization*, Vol. 24, pp. 325-332, 2002.

[6] Stander, N., Reichert, R., and Frand, T., "Optimization of Nonlinear Dynamical Problems Using Successive Linear Approximations," *8th AIAA/USAF/NASAISSMO Symposium on Multidisciplinary Analysis and Optimization*, Long Beach, CA, Sep. 6-8, 2000.

[7] Myers, R., H. and Montgomery, D., C, *Response Surface Methodology: Process and Product Optimization Using Designed Experiments*, John Wiley & Sons, Inc., 1995.

[8] Zadeh, P., M., and Toropov, V., "Multi-Fidelity Multidisciplinary Design Optimization based on Collaborative Optimization Framework," *9th AIAA/ISSMO Symposium on Multidisciplinary Analysis and Optimization*, AIAA-2002-5504.

[9] Hino, R., Yoshida, F., and Toropov, V., "Optimization of Blank Design for Deep Drawing Process Based on the Interaction of High and Low-Fidelity Models", *9th AIAA/ISSMO Symposium on Multidisciplinary Analysis and Optimization*, AIAA-2002-5564.

[10] Marduel, X., Tribes, C., and Trepanier, J., "Optimization using Variable Fidelity Solvers: Exploration of an Approximation Management Framework for Aerodynamic Shape Optimization," *9th AIAA/ISSMO Symposium on Multidisciplinary Analysis and Optimization*, AIAA-2002-5595.

[11] Markine, V., and Toropov, V., "Use of High and Low-Fidelity Models in Approximations for Design Optimization", *9th AIAA/ISSMO Symposium on Multidisciplinary Analysis and Optimization*, AIAA-2002-5651.

[12] Balabanov, V. O., "Development of Approximations for HSCT Wing Bending Material Weight using Response Surface Methodology," Ph.D. Dissertation, Virginia Polytechnic Institute and State University, 1997.

[13] LS-DYNA Version 960 Keyword User's Manual, Vol. I & II, Livermore Software Technology Corporation, Livermore, CA 94550, Mar. 2001.

[14] ABAQUS/Standard User's Manual, Version 6.4, Hibbit, Karlsson, and Sorensen, Inc, 1080 Main Street, Pawtucket, RI, 02860-4847, 2004.

[15] GENESIS Structural Analysis and Optimization Reference Manual, Version 7.2, Vanderplaats Research & Development, Inc., Colorado Springs, CO 80906, 2003.

[16] MSC.NASTRAN 2001 Quick Reference Guide, MSC Software Corporation, 815 Colorado Blvd, Los Angeles, CA 90041, 2001.

[17] DOT Design Optimization Tools Users Manual, Version 5.4 Vanderplaats Research & Development, Inc., Colorado Springs, CO 80906, 2004.

[18] VisualDOC Design Optimization Software Users Manual, Version 4.0, Vanderplaats Research & Development, Inc., Colorado Springs, CO 80906, 2004.

[19] Seely, F., B., and Smith, J., O., *Advanced Mechanics of Materials*, Second Edition, John Wiley & Sons, Inc., 1952.

[20] ABAQUS Example Problem Manual, Version 6.4, Hibbit, Karlsson, and Sorensen, Inc, 1080 Main Street, Pawtucket, RI, 02860-4847, 2004.